Supplementary Materials for

Synthesis and Characterization of Sterically Encumbered β-Ketoiminate Complexes of Iron(II) and Zinc(II)

David M. Granum,[a,b] Paul J. Riedel,[a,b] Joshua A. Crawford,[c] Thomas K. Mahle,[a] Chelsea M. Wyss,[a] Anastasia K. Begej,[a] Navamoney Arulsamy,[a] Brad S. Pierce,[c] and Mark P. Mehn*[a]

Supplementary Materials Available:

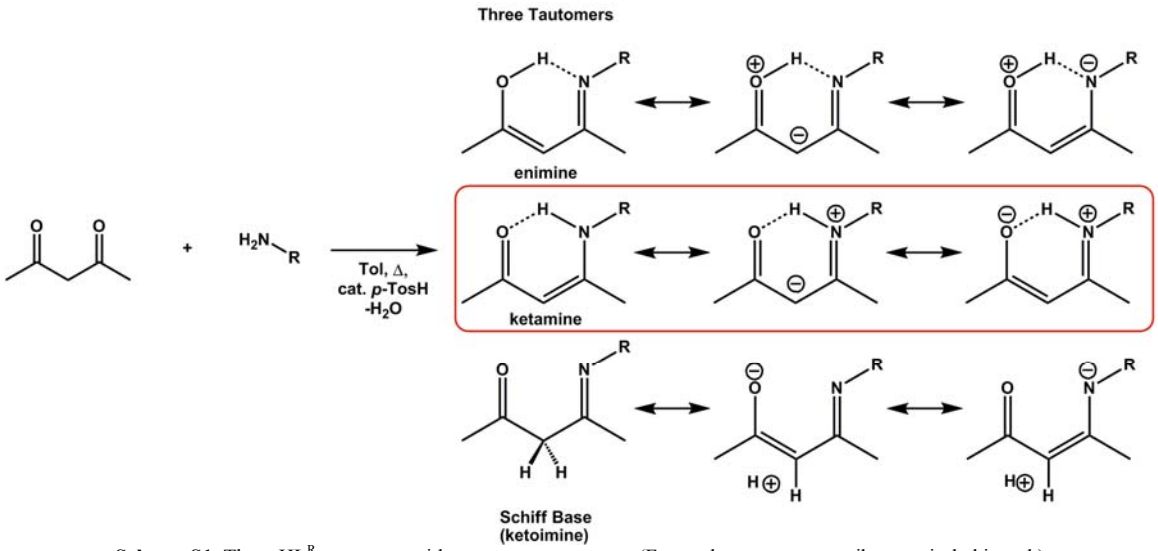

Scheme S1. Three HL^R tautomers with resonance structures. (Favored resonance contributors circled in red.)

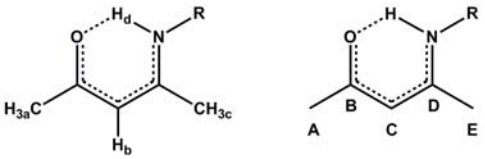

Scheme S2. Lettering for ^{1}H (lower case) and ^{13}C (upper case) NMR Assignments.

Table S1. ^{1}H NMR assignments for HL^{R} in $CDCl_3$ taken at room temperature.

Assignments	R = -iPr	R = -C_6H_5	R = -3,5-Me_2-C_6H_3	R = -2,6-iPr_2-C_6H_3	R= -2,4,6-Me_3-C_6H_2
a	1.94	1.98	2.08	2.12	2.10
b	4.87	5.07	5.15	5.21	5.19
c	1.91	1.86	1.98	1.63	1.63
d	10.79	12.40	12.41	12.05	11.84
e	3.67 (-C*H*(CH_3)$_2$)	-	-	-	-
f	1.20, 1.18 (-CH(*CH_3*)$_2$)	-	-	-	-
g	-	6.97 (*o*)	6.73 (*o*)	-	-
h	-	7.20 (*m*)	-	7.17 (*m*)	6.90 (*m*)
i	-	7.05 (*p*)	6.82 (*p*)	7.29 (*p*)	-
j	-	-	2.29 (-Me)	3.03 (-C*H*(CH_3)$_2$)	2.15 (-Me)
k	-	-		1.21, 1.15 (-CH(*CH_3*)$_2$)	2.28 (-Me)

Table S2. ^{13}C NMR assignments for HL^{R} in $CDCl_3$ taken at room temperature.

Assignments	R = -iPr	R = -C_6H_5	R = -3,5-Me_2-C_6H_3	R = -2,6-iPr_2-C_6H_3	R = -2,4,6-Me_3-C_6H_2
A	28	29	29	29	29
B	194	196	196	196	196
C	94	98	97	96	96
D	161	160	160	163	163
E	18	20	19	19	19
F	44 (-***C***H(CH_3)$_2$)	-	-	-	-
G	23 (-CH(***C***H_3)$_2$)	-	-	-	-
H	-	139 (*ipso*)	138 (*ipso*)	133 (*ipso*)	137 (*ipso*)
I	-	129 (o)	139 (o)	147 (o)	136 (o)
J	-	125 (*m*)	127 (*m*)	124 (*m*)	129 (*m*)
K	-	126 (*p*)	122 (*p*)	128 (*p*)	134 (*p*)
L	-	-	21 (-Me)	28 (-***C***H(CH_3)$_2$)	21 (-Me)
M	-	-	-	23, 25 (-CH(***C***H_3)$_2$)	18 (-Me)

Table S3. Comparison of bond distances in β-ketoiminate backbones .

	1 [$Fe(L^{iPr})_2$]		**2** [$Zn(L^{iPr})_2$]		**3a** [$Fe(HL^{dipp})_3(OTf)_2$]	**3b** [$Fe(L^{dipp})_2$]	**4** [$Zn(L^{dipp})_2$]
O-C_B	1.300(1)	1.293(1)	1.297(1)	1.292(1)	1.279(2), 1.277(2), 1.280(2)	1.289(1)	1.277(2), 1.279(1)
N-C_D	1.314(1)	1.314(1)	1.309(1)	1.309(1)	1.325(2), 1.324(2), 1.324(2)	1.321(1)	1.326(1), 1.328(1)
C_A-C_B	1.504(1)	1.506(2)	1.503(2)	1.506(2)	1.503(2), 1.495(2), 1.506(2)	1.501(2)	1.505(2), 1.507(2)
C_B-C_C	1.381(1)	1.380(1)	1.382(2)	1.380(2)	1.394(2), 1.394(2), 1.391(2)	1.380(2)	1.388(2), 1.390(2)
C_C-C_D	1.432(1)	1.434(1)	1.433(1)	1.435(2)	1.394(2), 1.394(2), 1.399(2)	1.416(1)	1.410(2), 1.414(2)
C_D-C_E	1.513(1)	1.513(1)	1.511(2)	1.514(2)	1.498(2), 1.498(2), 1.505(2)	1.507(1)	1.510(2), 1.513(2)

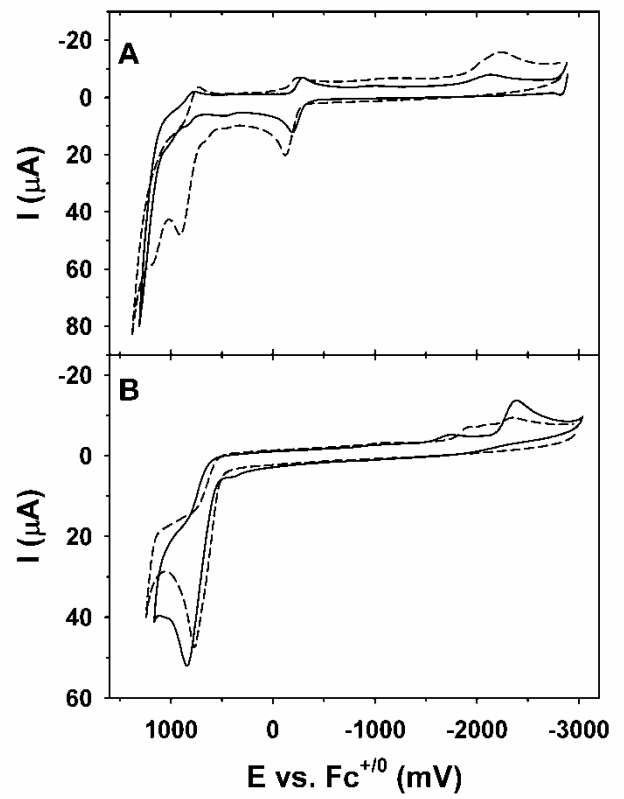

Figure S1. Cyclic voltammogram (CV) of A) 1.0 mM $[Fe(L^{iPr})_2]$ (– – – , top panel) and $[Fe(L^{dipp})_2]$ (—— top panel), and B) $[Zn(L^{iPr})_2]$ (– – – bottom panel) and $[Zn(L^{dipp})_2]$ (—— bottom panel) in THF at room temperature under nitrogen with 0.4 M $(^nBu_4N)(ClO_4)$ as supporting electrolyte.

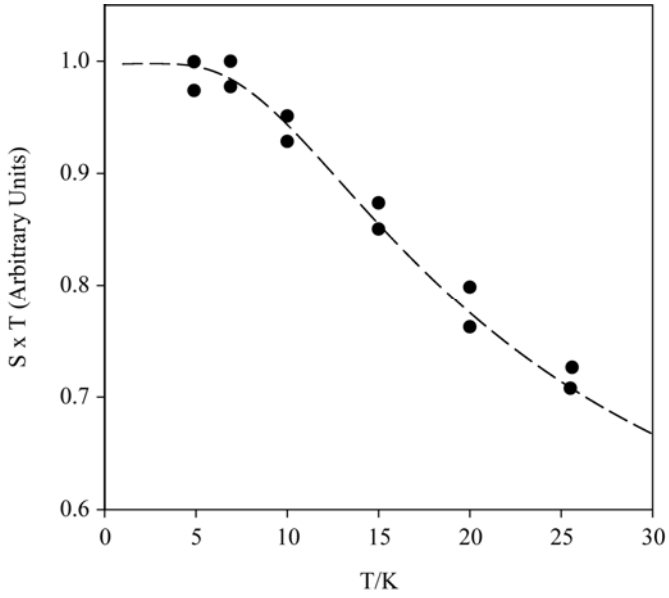

Figure S2. Normalized temperature dependence of the $S = 2$ signal **2b** (●) for the $[Fe(L^{dipp})_2]$ complex corrected for Curie Law dependence. The value for the axial zero-field splitting term (D = -7.1 ± 0.8 cm^{-1}) was determined by fitting (*dashed line*) the data to a Boltzman-dependent population distribution for a 3-level system (*equation S1, below*).

(eq. S1) $$Intensity \times T \sim n_s = \frac{g_i . e^{-\Delta E_i / k_b T}}{\sum_j g_j \cdot e^{-\Delta E_j / k_b T}} = \frac{(2S_i+1) \cdot e^{-DS^2_{z,i} / k_b T}}{\sum_j (2S_j+1) \cdot e^{-DS^2_{z,j} / k_b T}}$$

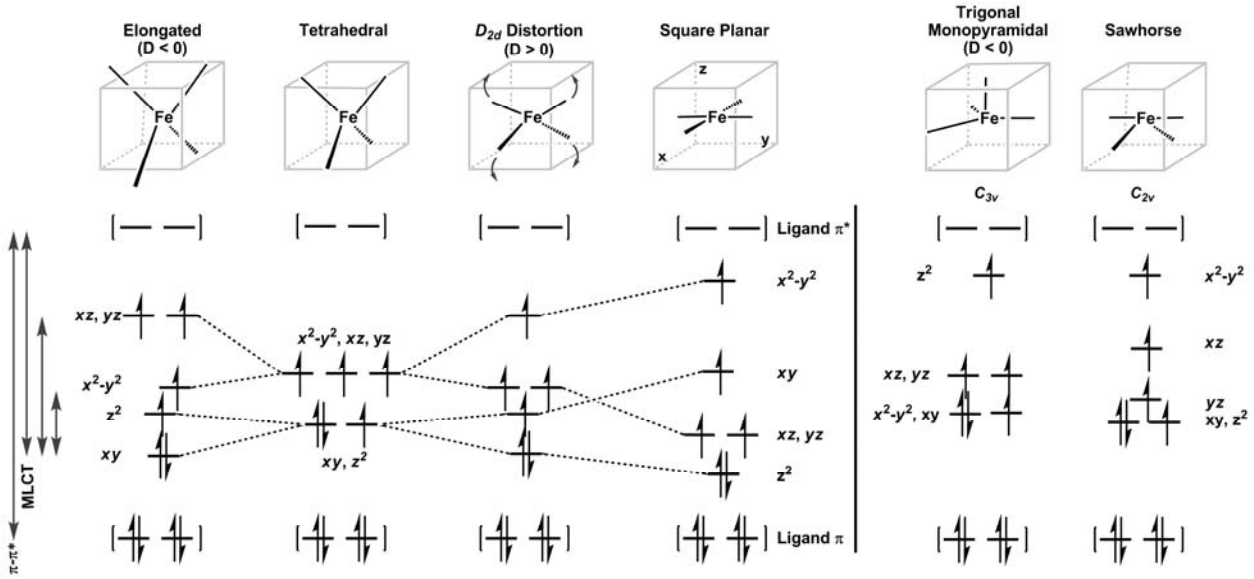

Figure S3. *Preliminary* molecular orbital splitting diagram for [Fe(L^{dipp})$_2$] showing descent from ideal tetrahedral symmetry. Adapted from E. I. Solomon, E. G. Pavel, K. E. Loeb, and C. Campochiaro, *Coord. Chem. Rev.*, 1995, **144**, 369-460 and S. Pulver, W. A. Froland, B. G. Fox, J. D. Lipscomb, and E. I. Solomon, *J. Am. Chem. Soc.*, 1993, **115**, 12409-12422. Please note that the coordinate axis is rotated by 45° from the typical depiction for a tetrahedral geometry (at the corners of the gray cube) to allow the correlation from square planar. The net result of this rotation is the interchange of the *d(x^2-y^2)* and *d(xy)* orbitals. Electronic transitions are shown as gray double headed arrows. The idealized splitting diagram for a trigonal monopyramidal ligand field under C_{3v} symmetry is taken from J. M. Mayer, D. L. Thorn, and T. H. Tulip, *J. Am. Chem. Soc.*, 1985, **107**, 7454-7462. The C_{2v} sawhorse splitting diagram comes from J. Cirera, E. Ruiz, and S. Alvarez, *Inorg. Chem.*, 2008, **47**, 2871-2889.

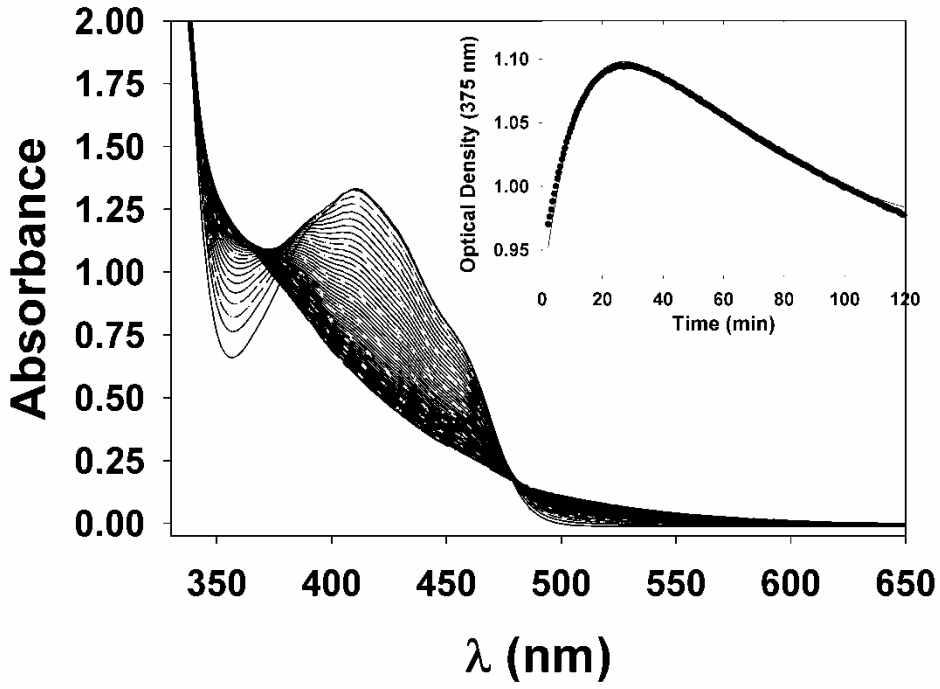

Figure S4. Electronic spectra of 0.613 mM [Fe(L^{iPr})$_2$] in THF upon exposure to O_2 (~10 mM assuming saturation of the THF solution, cycle time 2.5 min) for 2 hours. Inset: Representative kinetic trace following the growth and decay of the intensity at 375 nm.